Effects of Asymmetry Atmospheric Eddies on Spreading and Wander of Bessel–Gaussian Beams in Anisotropic Turbulence
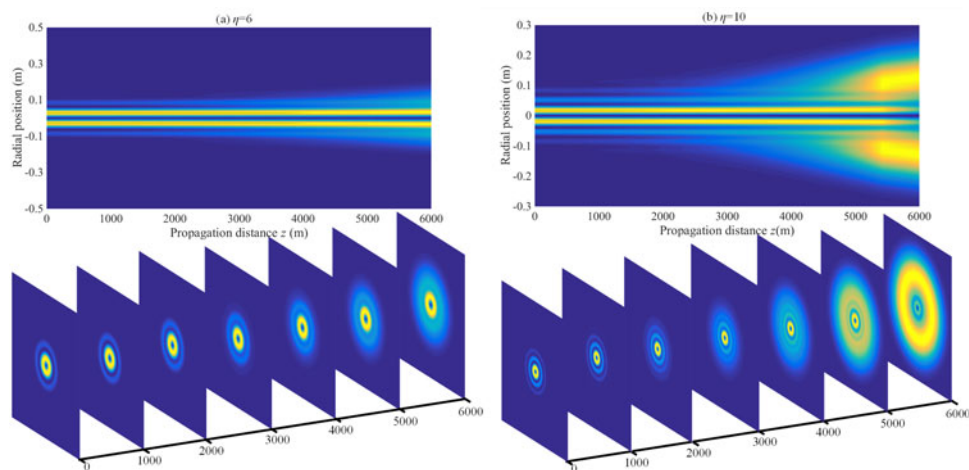
Mingjian Cheng
Lixin Guo, *Senior Member, IEEE*
Jiangting Li
Xu Yan
Ridong Sun
Yang You

Effects of Asymmetry Atmospheric Eddies on Spreading and Wander of Bessel–Gaussian Beams in Anisotropic Turbulence

Mingjian Cheng [ORCID],[1,2] **Lixin Guo,**[1] *Senior Member, IEEE*,
Jiangting Li [ORCID],[1] **Xu Yan,**[1] **Ridong Sun,**[1] **and Yang You**[3]

[1]School of Physics and Optoelectronic Engineering, Xidian University, Xi'an 710071, China
[2]State Key Laboratory of Pulsed Power Laser Technology, Hefei 230037, China
[3]Information and Communication Bureau of the Chinese Navy Staff, Beijing 100841, China

Abstract: The effects of asymmetry atmospheric eddies on the beam spreading and wander of Bessel–Gaussian (BG) beams in anisotropic turbulence are studied. Results show that turbulence anisotropy leads to the declines in both beam spreading and wander of BG beams in the atmosphere. A BG beam with larger beam shape parameter η has a narrower spot size in a short-distance range and a wider spot size in a long-distance range. The effective Rayleigh ranges of BG beams for every turbulent situation decrease with the beam shape parameter η. When η is larger than 10, atmospheric turbulence has a negligible effect on effective Rayleigh range. The effective Rayleigh range and beam spreading increase and beam wander decreases as topological charge increase. Beam spreading is mainly affected by turbulence inner-scale, and outer-scale evidently affects beam wander in the atmosphere.

Index Terms: Atmospheric turbulence, Bessel–Gaussian beams, orbital angular momentum, beam spreading, beam wander.

1. Introduction

Vortex beams with orbital angular momentum (OAM) have gained considerable interest and exhibited excellent potential applications in optical trapping [1], remote sensing [2], imaging systems [3], and communication systems [4]. A critical issue in extending the range of these systems is the capability to overcome turbulence-induced scintillation, modal degradation, beam spreading, and wander in the atmosphere. One recently explored approach to mitigating these turbulence effects is the adoption of non-diffracting vortex beams as the sources of these systems [5], [6]. Bessel–Gaussian (BG) beams, which are typical non-diffracting vortex beams [7], have the advantages of reducing scattering artefacts and increasing imaging quality and penetration in dense media [8], [9] due to their non-diffracting and self-healing behaviors. Thus far, the generation and

propagation properties of BG beams have been studied extensively theoretically and experimentally [10]–[18]. Nowadays, BG beams can be easily generated by using a suitable programmed spatial light modulator [10]. The transmission of OAM modes carried by BG beams in weak [11] and strong [12] turbulent atmosphere has been investigated and proven to be superior to that by Laguerre–Gaussian (LG) beams. The average intensity [13], [14] and M^2- factor [15] of BG beams in the atmosphere have been theoretically studied by utilizing the extended Huygens–Fresnel principle. The scintillation [16] and beam wander variance [17] of BG beams propagating in weak turbulent media have been evaluated with the use of integrated moments. Yuan [18] derived an analytical formula for the beam wander variance of BG beams propagating through turbulent atmosphere. As is known, beam wander is caused mostly by large-scales atmospheric eddies near the transmitter, where the beam size has not expanded much beyond its free-space size. Thus, Andrews and Phillips [19] used the free space beam radius in the filter function of beam wander variance model. Many academics employed long–term beam radius in the turbulence rather than free space beam radius, when calculating the filter function in the model of beam wander variance. Consequently, the effect of beam wander was considered twice and underestimated. The same problem also exists in the calculation of the beam wander variance of BG beams in [18].

The Kolmogorov spectrum is widely used in atmospheric turbulence modeling [19]. However, recent experimental results [20], [21] have indicated that optical turbulence structure in stably layered atmosphere (e.g., in free atmosphere or near the ground) is inhomogeneous, anisotropic, and not consistent with the Kolmogorov spectrum model. Hence, several anisotropic non-Kolmogorov spectrum models [22], [23] have been proposed to describe the real turbulence behavior of laser beams in the atmosphere. The effects of asymmetry atmospheric eddies on the transmission of OAM modes carried by BG beams in an anisotropic non-Kolmogorov turbulent atmosphere were studied, and the results indicated that anisotropic turbulence produces a considerable weaker effect than isotropic turbulence [24]. To the best of our knowledge, the beam spreading and wander of BG beams in an anisotropic non-Kolmogorov turbulent atmosphere has not been studied. An understanding of the transmission effects for BG beams in an anisotropic turbulent atmosphere is an important complement for the practical design of free-space optical vortex communication systems.

In this study, the beam wander variance model in anisotropic turbulence with the asymmetric atmospheric eddies in the orthogonal xy-plane throughout the path has been established and adopted to study the effects of asymmetry atmospheric eddies on beam wander variance of BG beams. The analytic expressions of the long-term beam radius, and effective Rayleigh range of BG beams in the atmosphere are also obtained. We explore the influence of turbulent parameters, topological charge and beam shape parameter on the changes in the effective Rayleigh range, beam spreading and wander of BG beams in the atmosphere.

2. Theoretical Analysis

Considering the asymmetric property of atmospheric eddies and finite turbulence inner- and outer-scales effects, the spatial power spectrum model of refractive-index fluctuations in anisotropic non-Kolmogorov turbulence is given by [24]:

$$\phi_n(\kappa) = A(\alpha) C_n^2 \xi_x \xi_y \exp\left[-\left(\xi_x^2 \kappa_x^2 + \xi_y^2 \kappa_y^2 + \kappa_z^2\right)/\kappa_l^2\right]\left(\xi_x^2 \kappa_x^2 + \xi_y^2 \kappa_y^2 + \kappa_z^2 + \kappa_0^2\right)^{-\alpha/2}, \qquad (1)$$

where $\kappa = \sqrt{\kappa_x^2 + \kappa_y^2 + \kappa_z^2}$, ξ_x and ξ_y are two anisotropy parameters representing scale-dependent stretching along the x and y directions, respectively. If $\xi_x = \xi_y = 1$, (1) reduces to a conventional isotropic turbulent spectrum, $\kappa_l = c(\alpha)/l_0$, $\kappa_0 = 2\pi/L_0$, l_0 is turbulent inner-scale and L_0 is outer-scale, $A(\alpha)$ and $c(\alpha)$ are given by,

$$A(\alpha) = \Gamma(\alpha - 1)\cos(\pi\alpha/2)/\left(4\pi^2\right), \qquad (2)$$

$$c(\alpha) = \left\{A(\alpha)\Gamma\left[(5 - \alpha)/2\right]2\pi/3\right\}^{1/(\alpha-5)}, \qquad (3)$$

where $\Gamma(x)$ is the Gamma function; α is the power spectrum index with $3 < \alpha < 4$; C_n^2 is a generalized structure parameter with units $m^{3-\alpha}$.

The complex amplitude of BG beams at the source plane (i.e., $L = 0$) can be expressed as [24]:

$$E_l(\mathbf{r}, 0) = \exp\left(-r^2/w_0^2\right) J_l(\eta r/w_0) \exp(-il\varphi), \tag{4}$$

where $\mathbf{r} = (r, \varphi)$ is the two-dimensional position vector at the source plane, l is the topological charge associated to BG beams; φ is azimuthally angle; beam width w_0 denotes the radius at which the field amplitude falls to $1/e$; $\eta = k\sin\theta_0 w_0$ is a constant that determines the beam profile, $k = 2\pi/\lambda$ is the wave number of the incident wavelength λ, θ_0 is the angle of the conical wave that forms the Bessel beam, and $J_m(x)$ is the Bessel function of first kind with m order.

In free space without turbulence, the complex amplitude of BG beams, under the paraxial approximation, can be expressed as [24],

$$E_l^{\text{free}}(\rho, L) = \frac{1}{q} J_l\left(\frac{\eta\rho}{qw_0}\right) \exp\left(ikL - \frac{\rho^2}{qw_0^2} + \frac{\eta^2}{4q} - \frac{\eta^2}{4}\right) \exp(-il\phi), \tag{5}$$

where $q = 1 + iL/z_0$, and $z_0 = kw_0^2/2$ is the Rayleigh range.

Based on the second-order moments of BG beams [15], we can write the mean-squared long-term beam radius of BG beams propagating through atmospheric turbulence as,

$$W_{\text{LT}}^2(L) = A + BL^2 + CL^3, \tag{6}$$

with

$$A = \frac{w_0^2}{2} + \frac{\eta^2 w_0^2}{8}\left[\frac{I_{l+1}(\eta^2/4) + I_{l-1}(\eta^2/4)}{2I_l(\eta^2/4)} - 1\right], \tag{7}$$

$$B = \frac{2}{k^2 w_0^2}\left[1 + \frac{\eta^2}{4} + \frac{I_{l+1}(\eta^2/4) + I_{l-1}(\eta^2/4)}{8I_l(\eta^2/4)/\eta^2}\right], \tag{8}$$

$$C = \frac{4}{3}\pi^2 \int_0^\infty \kappa^3 \phi_n(\kappa)\, d\kappa. \tag{9}$$

Invoking the Markov approximation, which implies that the refraction index is delta-correlated at any pair of points located along the propagation direction, κ_z in (1) can be ignored. We change the spectrum into an isotropic one by following change of variables [25],

$$\kappa_x = \frac{q_x}{\xi_x} = \frac{q\cos\theta}{\xi_x}, \kappa_y = \frac{q_y}{\xi_y} = \frac{q\sin\theta}{\xi_y}, q = \sqrt{q_x^2 + q_y^2}, d\kappa_x d\kappa_y = \frac{dq_x dq_y}{\xi_x\xi_y} = \frac{q\,dq\,d\theta}{\xi_x\xi_y}. \tag{10}$$

The spectrum (1) becomes,

$$\phi_n(q, 0) = \frac{A(\alpha) C_n^2 \xi_x \xi_y}{\left(q^2 + \kappa_0^2\right)^{\alpha/2}} \exp\left(-\frac{q^2}{\kappa_l^2}\right). \tag{11}$$

By substituting (11) into (9), and utilizing the Markov approximation, yields,

$$C = \frac{\xi_x^2 + \xi_y^2}{\xi_x^2 \xi_y^2} \frac{A(\alpha)\pi^2 C_n^2}{3(\alpha - 2)}\left[\kappa_l^{2-\alpha}\left(2\kappa_0^2 - 2\kappa_l^2 + \alpha\kappa_l^2\right) \Gamma\left(2 - \frac{\alpha}{2}, \frac{\kappa_0^2}{\kappa_l^2}\right) \exp\left(\frac{\kappa_0^2}{\kappa_l^2}\right) - 2\kappa_0^{4-\alpha}\right], \tag{12}$$

with $\Gamma(x, y)$ being the incomplete Gamma function.

The effective Rayleigh range used for characterizing a collimated range of laser beams propagation through atmospheric turbulence is defined as the distance at which the mean-squared long-term beam radius is twice as large as its initial value, i.e., $W_{\text{LT}}^2(z_{\text{RT}}) = 2A$ [26]. Among the three solutions of this cubic equation, there is only one-real solution, which represents the effective Rayleigh range z_{RT} of BG beam in the atmospheric turbulence,

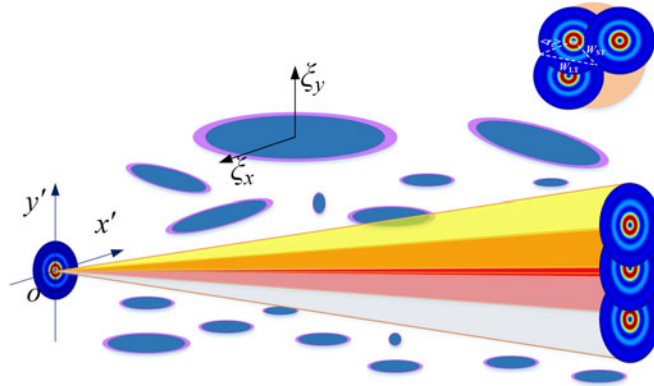$$z_{\text{RT}} = \left[Y + B^2/Y - B\right]/(3C), \tag{13}$$

Fig. 1. Schematic of BG beams propagation in anisotropic turbulence.

with

$$Y = \left[13.5A\,C^2 - B^3 + 1.5C\sqrt{81A^2C^2 - 12A\,B^3}\right]^{1/3}. \tag{14}$$

As a BG beam propagates through a random medium, its instantaneous center becomes randomly displaced in the receiver plane, which produces the beam spreading and wander (see Fig. 1). Beam wander acts like a random tilt at the transmitter plane, can be described statistically by the variance in this displacement. The general expression of the beam wander variance is given by [19]:

$$\langle r_c^2 \rangle = 4\pi^2 k^2 W_{FS}^2(L) \int_0^L \int_0^\infty \kappa \phi_n(\kappa) H_{LS}(\kappa, z) \left\{ 1 - \exp\left[-\left(1 - \frac{z}{L}\right)^2 \frac{2L^2\kappa^2}{k^2 W_{FS}^2(L)} \right] \right\} d\kappa dz, \tag{15}$$

where W_{FS} is free-space beam radius, which is obtained from (6) by setting $C = 0$. Large-scale filter function $H_{LS}(\kappa, z)$ has the form as,

$$H_{LS}(\kappa, z) = \exp\left[-\kappa^2 W_{FS}^2(z)\right], \tag{16}$$

Note that we adopt the free-space beam radius rather than long-term beam radius in the large-scale filter function. Using the long-term beam radius means that beam wander is already known and the effect of beam wander will be considered twice, which contradicts the reality and underestimate the effect of atmospheric turbulence on the beam wander.

Beam wander is a refractive effect, mostly caused by the refraction of large-scale turbulence cells near the transmitter. Thus, the diffraction effect can be neglected, (15) can be simplified by applying the geometrical optics approximation,

$$1 - \exp\left[-\left(1 - \frac{z}{L}\right)^2 \frac{2L^2\kappa^2}{k^2 W_{FS}^2(L)} \right] \approx \left(1 - \frac{z}{L}\right)^2 \frac{2L^2\kappa^2}{k^2 W_{FS}^2(L)}, \tag{17}$$

Substitute (11) and (16), (17) into (15), we have,

$$\langle r_c^2 \rangle = 4\pi L^2 A(\alpha) \tilde{C}_n^2 \int_0^L \int_0^{2\pi} \int_0^\infty \left(\frac{\cos^2\theta}{\xi_x^2} + \frac{\sin^2\theta}{\xi_y^2} \right) \frac{(1 - z/L)^2 q^3}{\left(q^2 + \kappa_0^2\right)^{\alpha/2}}$$

$$\times \exp\left\{ -\left[\frac{1}{\kappa_l^2} + \left(\frac{\cos^2\theta}{\xi_x^2} + \frac{\sin^2\theta}{\xi_y^2} \right) W_{FS}^2(z) \right] q^2 \right\} dq d\theta dz. \tag{18}$$
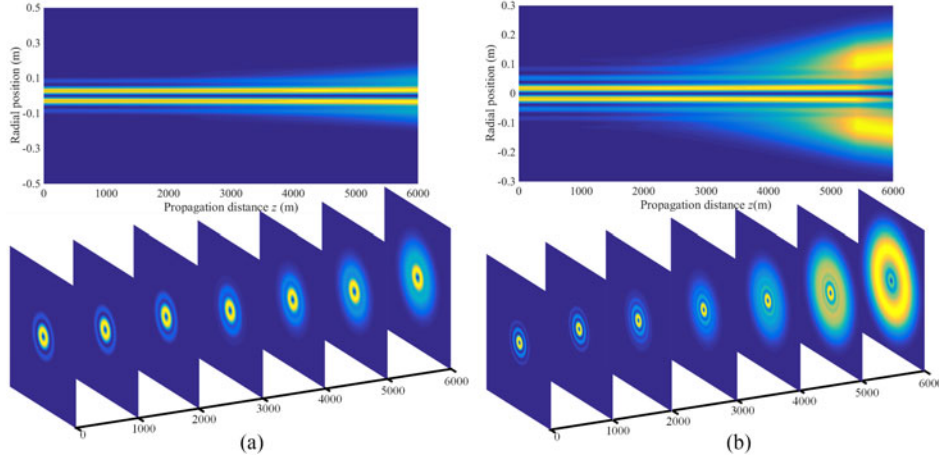
Fig. 2. Side-view propagation and intensity distributions of BG beams in free space for different η. (a) $\eta = 6$. (b) $\eta = 10$.

Utilizing integral calculation, the beam wander variance of BG beams propagation through anisotropic turbulence can be written as,

$$\langle r_c^2 \rangle = \frac{2\pi A\,(\alpha)\,C_n^2 L^2 \kappa_0^{4-\alpha}}{\alpha - 2} \int_0^L \int_0^{2\pi} \left(\frac{\cos^2\theta}{\xi_x^2} + \frac{\sin^2\theta}{\xi_y^2} \right) \left(1 - \frac{z}{L} \right)^2$$

$$\times \left[D^{\alpha/2-2} \exp(D)\,(2D - 2 + \alpha)\,\Gamma(2 - \alpha/2, D) - 2 \right] d\theta dz, \tag{19}$$

where $D = \kappa_0^2/\kappa_l^2 + (\cos^2\theta/\xi_x^2 + \sin^2\theta/\xi_y^2)W_{FS}^2(z)\kappa_0^2$.

Following Fante [27], the short-term beam radius for a BG beam in the turbulent atmosphere is defined by:

$$W_{ST} = \sqrt{W_{LT}^2 - \langle r_c^2 \rangle}. \tag{20}$$

3. Numerical Discussion

This section presents our investigation on the influences of asymmetry atmospheric eddies and source parameters on beam spreading and wander of BG beams in anisotropic turbulence. The following parameter values are assumed unless otherwise specified: OAM mode $l = 1$; beam width $w_0 = 0.1\,\text{m}$; beam shape parameter $\eta = 6$; wavelength $\lambda = 1550\,\text{nm}$; anisotropy coefficients $\xi_x = 20$, $\xi_y = 1.3$; power spectrum index $\alpha = 3.2$; turbulence outer-scale $L_0 = 1\,\text{m}$, inner-scale $l_0 = 1\,\text{cm}$; turbulent structure parameter $C_n^2 = 10^{-14}\,\text{m}^{3-\alpha}$; and propagation distance $L = 5\,\text{km}$. The parameters adopted in this work are set as examples for theoretical analysis purposes; other values can also be adopted.

The influence of beam shape parameter η on the side-view propagation of BG beams in free space is depicted in Fig. 2. We set η as 6 and 10. We choose seven observing planes at different propagation distances (0, 2, 3, 4, 5 and 6 km), to investigate the changes in intensity distributions of BG beams along the propagation path. For a fixed Gaussian beam width w_0, raising the value of η causes BG beam to be more of a pure Bessel beams by pulling the zero crossings towards on-axis. While if reducing the value of η, the Gaussian exponential term will dominate and Bessel appearance is gradually removed from the intensity profile. When η approaches zero, the Gaussian profile is much narrower than the central lobe of Bessel function, BG beam will transform into a LG beam without outer rings. The propagation of BG beams can be divided into two stages: in the first stage, the multi-ring intensity pattern and spot size are maintained well; in the second stage, the spot size increases sharply and the multi-ring intensity evolves into a single-ring profile with the
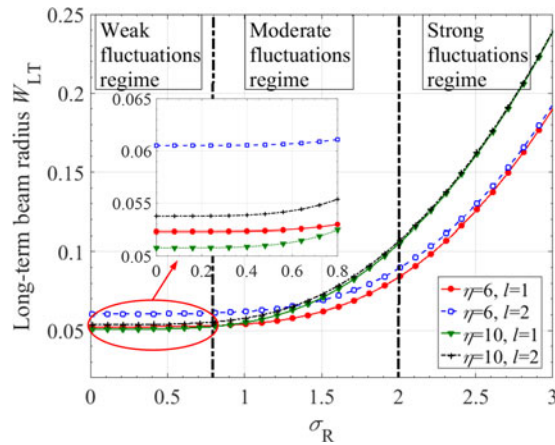
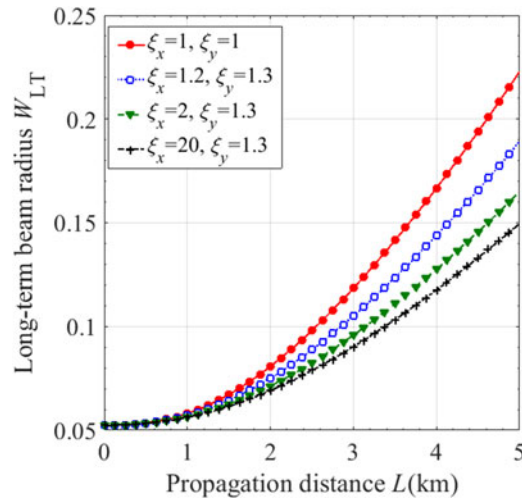Fig. 3. Long-term beam spreading of BG beams in anisotropic turbulence versus σ_R for different η and l.

Fig. 4. Long-term beam spreading of BG beams in anisotropic turbulence versus L for different ξ_x and ξ_y.

increase of propagation distance. The value of η has a significant effect on the demarcation point between these two stages.

Fig. 3 plots the long-term beam radius W_{LT} of BG beams in an anisotropic turbulence versus turbulence strength (Rytov variance $\sigma_R^2 = 1.23 C_n^2 k^{3-\alpha/2} L^{\alpha/2}$) from 0 to 3, where the effects of different beam shape parameters $\eta = 6$ and 10 and different topological charges $l = 1$ and 2 are considered. W_{LT} of a BG beam is sensitive to the changes in associated η and l. An increase in the value of l generally leads to evident beam spreading in regions with weak-to-moderate fluctuations. However, the effect of l on long-term beam spreading in a strong-turbulence region can be ignored. A BG beam with a large η has a narrow spot size in weak-to-moderate fluctuation regimes or short-distance transmission. Conversely, an increase in η leads to increasingly beam spreading in strong fluctuation regime.

An evaluation of the long-term beam radius W_{LT} of BG beams in anisotropic turbulence along L for different anisotropy coefficients ξ_x and ξ_y cases is detailed in Fig. 4. W_{LT} of a BG beam increases with L or turbulence strength. A comparison of the long-term beam spreading in isotropic turbulence ($\xi_x \neq 1$ or $\xi_y \neq 1$) and anisotropic turbulence ($\xi_x = \xi_y = 1$) show that anisotropic turbulence produces a weaker effect on beam spreading than isotropic turbulence does. The beam
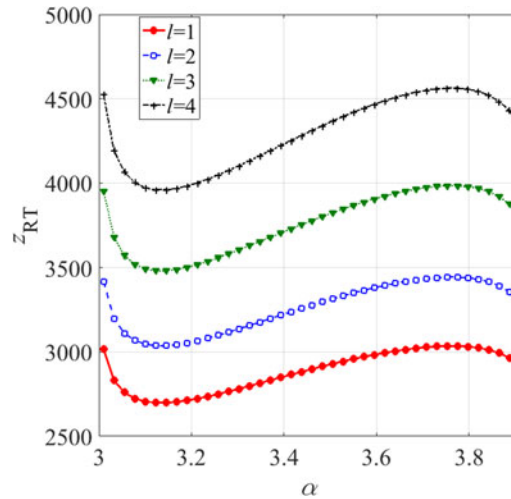
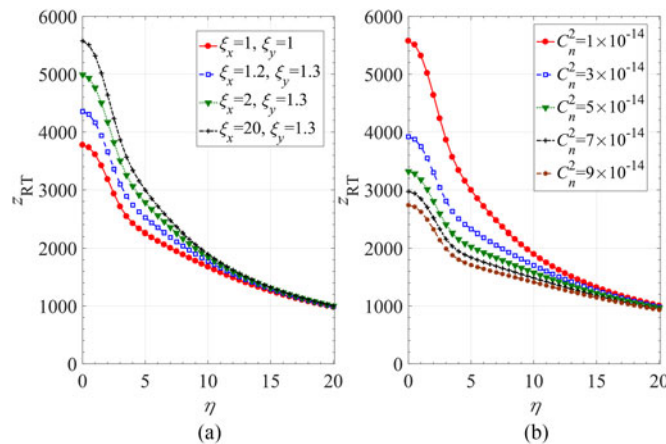Fig. 5. Effective Rayleigh ranges z_{RT} of BG beams in anisotropic turbulence versus α for different l.

Fig. 6. Effective Rayleigh ranges z_{RT} of BG beams in anisotropic turbulence versus η for different ξ_x, ξ_y (a) and C_n^2 (b).

spreading effect in anisotropic turbulence is generally suppressed along with an enhancement of the anisotropy coefficients. The reduction of the long-term beam spread because of the increase of anisotropy coefficients is understandable, since the anisotropic atmospheric eddies can change the focusing properties of the turbulence, and the divergence directionality of the beam will be suppressed.

Fig. 5 demonstrates the dependence of the effective Rayleigh range z_{RT} of BG beams on l in anisotropic turbulence as a function of the power spectrum index α. Here, we selected l value ranges of 1, 2, 3 and 4. The curves of z_{RT} of BG beams with varying l follow similar trends, but different values are obtained. The larger the value of l, the larger z_{RT} in the atmosphere. z_{RT} decreases with the initial increase in α and returns to the growth region after reaching the minimum value at approximately $\alpha = 3.1$. z_{RT} begins to decrease again when α is larger than 3.8. This result is consistent with that of the wave structure function in non-Kolmogorov turbulence.

Fig. 6 shows the plots of z_{RT} of BG beams in anisotropic turbulence against beam shape parameter η from 0 to 20, where the effects of different ξ_x and ξ_y and turbulent structure parameter C_n^2 are considered. The BG beams have larger z_{RT} under anisotropic turbulence than under isotropic turbulence. The turbulence strength enhances with the turbulent structure parameter and weakens
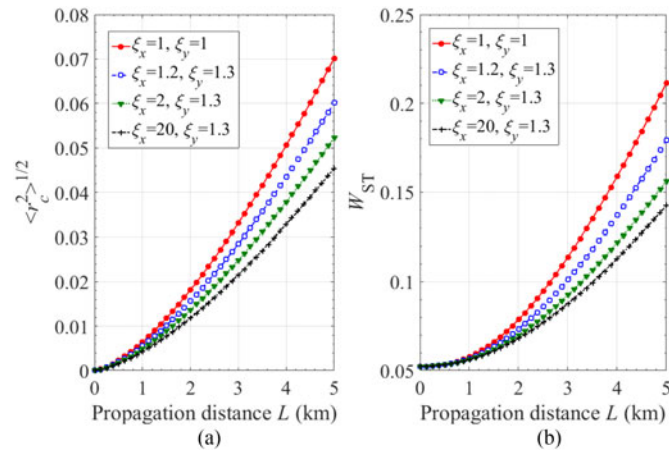
Fig. 7. Rms beam wander variance (a) and short-term beam spreading (b) of BG beams in anisotropic turbulence versus L for different ξ_x and ξ_y.
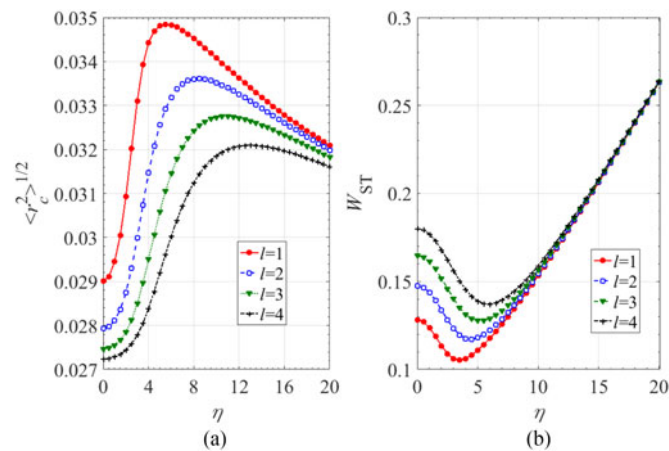

Fig. 8. Rms beam wander variance (a) and short-term beam spreading (b) of BG beams in anisotropic turbulence versus η for different l.

with the anisotropy coefficients, thus resulting in a reduced z_{RT}. z_{RT} of BG beams for every turbulent situation decrease with an increase in η. When η is larger than 10, turbulence has a negligible influence on z_{RT} of BG beams in strong turbulent fluctuation regime. This is because that z_{RT} of these BG beams are limited to 2000 m, where BG beams are more impacted by their own structural characteristic.

The influence of the anisotropy coefficients ξ_x and ξ_y on the Rms beam wander variance $\langle r_c^2 \rangle^{1/2}$ and short-term beam radius W_{ST} of BG beams in anisotropic turbulence as a function of L are presented in Fig. 7. The beam wander and short-term beam spreading of BG beams increase with L. Anisotropic turbulence with greater values of ξ_x and ξ_y produces a smaller effect on beam spreading and wander than isotropic turbulence does. It is known that beam wander is caused mostly by the refraction effects of atmospheric eddies. The anisotropy of turbulence will lead to a weaker refraction effect than in the isotropic turbulence medium, thus, enhancing turbulent anisotropy will contribute to a smaller beam wander. When BG beams are propagating in weak fluctuation or short distance regimes, the effect of the anisotropy coefficients on the beam spreading and wander are trivial.

Fig. 8 illustrates the effect of topological charge l on $\langle r_c^2 \rangle^{1/2}$ and W_{ST} of BG beams in anisotropic turbulence as a function of η by setting $l = 1, 2, 3$, and 4. The changes in η and l have evident effects
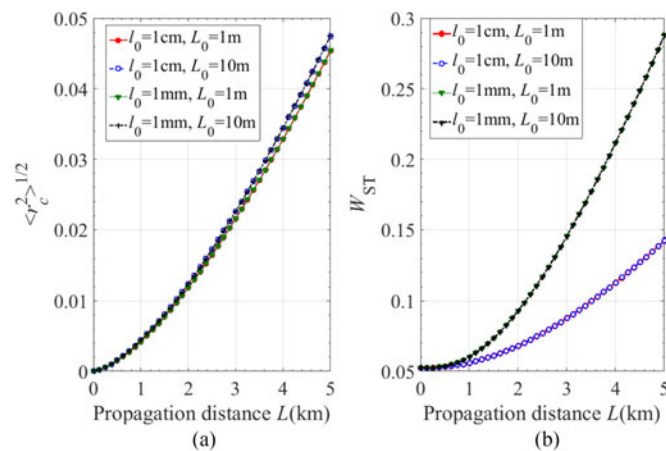
Fig. 9. Rms beam wander variance (a) and short-term beam spreading (b) of BG beams in anisotropic turbulence versus L for different l_0 and L_0.

on the beam wander and spreading of BG beams in the atmosphere. BG beams with different l have varying spot sizes in the turbulent atmosphere, thereby resulting in beam wander with different strengths. An increase in the value of l leads to a decrease in beam wander and an increase in beam spreading, when η is smaller than 10. Beam wander of BG beams strengthen with initial increasing phase of η and begin to decline after reaching the maximum value. Such trend of beam wander of a BG beam against η in the atmosphere is caused by its spatial structure (a central core surrounded by a set of concentric bright and dark rings). The changing trend of the curves for short-term beam radius against η contradicts that of beam wander.

Fig. 9 details the evaluation of $\langle r_c^2 \rangle^{1/2}$ and W_{ST} of BG beams in anisotropic turbulence along L for different L_0 and l_0 cases. Beam wander mainly arises from the refraction effect of the large-scale turbulence cells near the transmitter, and the refraction effect is noticeable in the atmospheric with large outer-scale. Outer-scale turbulence effect plays an important role in determining the strength of beam wander, and a negligible role in short-term beam spreading. However, inner-scale has a more significant effect on short-term beam spreading than beam wander. The smaller inner-scale, the more noticeable diffraction effect, thereby resulting in increased short-term beam radius. The value of W_{ST} is considerably larger than that of $\langle r_c^2 \rangle^{1/2}$. Consequently, W_{LT} is also mainly affected by inner-scale.

4. Conclusion

In conclusion, we quantitatively investigated the effects of asymmetry atmospheic eddies on beam spreading and wander of BG beams in anisotropic turbulence. Turbulence anisotropy characteristic led to the declines in beam spreading and wander, and an increase in effective Rayleigh ranges of BG beams in the atmosphere. The parameters selection of BG beams depended on the application scenario. BG beams were more suitable for short-range application scenarios such as undersea laser communication and remote sensing than LG beams. For long-distance transmission, BG beams had a worse performance than LG beams, because the effective Rayleigh ranges of BG beams were limited to 2 km. The amplitude and phase profiles of BG beam could be tuned by modifying its topological charge l, beam shape parameter η, and beam width w_0. BG beams with large η had narrow and wide spot sizes in short- and long-distance ranges, respectively. The effects of η on beam wander were contrary to those on beam spreading. The effective Rayleigh ranges for every turbulent situation decreased with η. When η was larger than 10, atmospheric turbulence had a negligible impact on the effective Rayleigh range. As l increased, the effective Rayleigh range and beam spreading increased and beam wander decreased. Turbulence inner-scale played an

important role in determining the strength of beam spreading and outer-scale evidently affected beam wander.

Acknowledgment

The authors would like to thank the anonymous reviewers for their valuable suggestions.

References

[1] M. P. MacDonald, L. Paterson, K. Volke-Sepulveda, J. Arlt, W. Sibbett, and K. Dholakia, "Creation and manipulation of three-dimensional optically trapped structure," *Science*, vol. 296, no. 5570, pp. 1101–1103, May 2002.

[2] M. P. J. Lavery, F. C. Speirits, S. M. Barnett, and M. J. Padgett, "Detection of a spinning object using light's orbital angular momentum," *Science*, vol. 341, no. 6145, pp. 537–540, Aug. 2013.

[3] L. Torner, J. P. Torres, and S. Carrasco, "Digital spiral imaging," *Opt. Exp.*, vol. 13, no. 3, pp. 873–881, Feb. 2005.

[4] S. Mi, T. Wang, G. Jin, and C. Wang, "High-capacity Quantum Secure Direct Communication with Orbital Angular Momentum of photons," *IEEE Photon. J.*, vol. 7, no. 5, Oct. 2015, Art. no. 7600108.

[5] M. Cheng, L. Guo, J. Li, and Y. Zhang, "Channel Capacity of the OAM-Based Free-Space Optical Communication Links with Bessel–Gauss Beams in Turbulent Ocean," *IEEE Photon. J.*, vol. 8, no. 1, Feb. 2016, Art. no. 7901411.

[6] S. Li and J. Wang, "Adaptive free-space optical communications through turbulence using self-healing Bessel beams," *Sci. Rep.*, vol. 7, Feb. 2017, Art. no. 43233.

[7] J. Durnin and J. J. Miceli, "Diffraction-free beams," *Phys. Rev. Lett.*, vol. 58, no. 15, pp. 1499–1501, Apr. 1987.

[8] F. Fahrbach, P. Simon, and A. Rohrbach, "Microscopy with self-reconstructing beams," *Nature Phot.*, vol. 4, no. 11, pp. 780–785, Sep. 2010.

[9] F. Fahrbach and A. Rohrbach, "Propagation stability of self-reconstructing Bessel beams enables contrast-enhanced imaging in thick media," *Nature Commun.*, vol. 3, Jan. 2012, Art. no. 632.

[10] N. Chattrapiban, E. Rogers, D. Cofield, W. Hill, and R. Roy, "Generation of nondiffracting Bessel beams by use of a spatial light modulator," *Opt. Lett.*, vol. 28, no. 22, pp. 2183–2185, Nov. 2003.

[11] J. Ou *et al.*, "Spreading of spiral spectrum of Bessel–Gaussian beam in non-Kolmogorov turbulence," *Opt. Commun.*, vol. 318, pp. 95–99, Jan. 2014.

[12] Y. Li, Y. Zhang, D. Wang, L. Shan, M. Chao, and Y. Zhao, "Statistical distribution of the OAM states of Bessel–Gaussian–Schell infrared beams in strong turbulent atmosphere," *Infrared Phys. Techn.*, vol. 76, pp. 569–573, May 2016.

[13] H. Eyyuboğlu, "Propagation of higher order Bessel–Gaussian beams in turbulence," *Appl. Phys. B*, vol. 88, no. 2, pp. 259–265, Jul. 2007.

[14] K. Zhu, G. Zhou, X. Li, X. Zheng, and H. Tang, "Propagation of Bessel–Gaussian beams with optical vortices in turbulent atmosphere," *Opt. Exp.*, vol. 16, no. 26, pp. 21315–21320, Dec. 2008.

[15] K. Zhu, S. Li, Y. Tang, Y. Yu, and H. Tang, "Study on the propagation parameters of Bessel–Gaussian beams carrying optical vortices through atmospheric turbulence," *J. Opt. Soc. Amer. A*, vol. 29, no. 3, pp. 251–257, Mar. 2012.

[16] H. Eyyuboglu, E. Sermutlu, Y. Baykal, Y. Cai, and O. Korotkova, "Intensity fluctuations in J-Bessel-Gaussian beams of all orders propagating in turbulent atmosphere," *Appl. Phys. B*, vol. 93, pp. 605–611, Oct. 2008.

[17] I. P. Lukin, "Random displacement of the Bessel–Gaussian beam in turbulent atmosphere," *Proc. SPIE*, vol. 9292, Nov. 2014, Art. no. 929220.

[18] Y. Yuan *et al.*, "Beam wander relieved orbital angular momentum communication in turbulent atmosphere using Bessel beams," *Sci. Rep.*, vol. 7, Feb. 2017, Art. no. 42276.

[19] L. C. Andrews and R. L. Phillips, *Laser Beam Propagation through Random Media*, 2nd ed. Bellingham, WA, USA: SPIE, 2005.

[20] L. Biferale and I. Procaccia, "Anisotropy in turbulent flows and in turbulent transport," *Phys. Rep.*, vol. 414, no. 2, pp. 43–164, Jul. 2005.

[21] G. M. Grechko, A. S. Gurvich, V. Kan, S. V. Kireev, and S. A. Savchenko, "Anisotropy of spatial structures in the middle atmosphere," *Adv. Space Res.*, vol. 12, no. 10, pp. 169–175, Oct. 1992.

[22] I. Toselli, B. Agrawal, and S. Restaino, "Light propagation through anisotropic turbulence," *J. Opt. Soc. Amer. A*, vol. 28, no. 3, pp. 483–488 Mar., 2011.

[23] I. Toselli, "Introducing the concept of anisotropy at different scales for modeling optical turbulence," *J. Opt. Soc. Amer. A*, vol. 31, no. 8, pp. 1868–1875, Aug. 2014.

[24] C. Sheppard, "Beam duality, with application to generalized Bessel–Gaussian, and hermite- and Laguerre–Gaussian beams," *Opt. Exp.*, vol. 17, no. 5, pp. 3690–3697, Feb. 2009.

[25] M. Cheng, L. Guo, J. Li, and Q. Huang, "Propagation properties of an optical vortex carried by a Bessel–Gaussian beam in anisotropic turbulence," *J. Opt. Soc. Amer. A*, vol. 33, no. 8, pp. 1442–1450, Jul. 2016.

[26] A. E. Siegman, *Laser*. Mill Valley, CA, USA: Univ. Science, 1986.

[27] R. L. Fante, "Electromagnetic beam propagation in turbulent media," *Proc. IEEE*, vol. 63, no. 12, pp. 1669–1692, Dec. 1975.